Available online at www.sciencedirect.com
SCIENCE DIRECT®
International Journal of Heat and Fluid Flow 24 (2003) 762–773
International Journal of HEAT AND FLUID FLOW
www.elsevier.com/locate/ijhff

Heat transfer to viscoplastic materials flowing axially through concentric annuli

Edson J. Soares, Mônica F. Naccache, Paulo R. Souza Mendes *

Department of Mechanical Engineering, Pontifícia Universidade Católica, Rua Marquês de São Vicente 225, Rio de Janeiro, RJ 22453-900, Brazil

Received 9 October 2002; accepted 9 April 2003

Abstract

Heat transfer in the entrance-region laminar axial flow of viscoplastic materials inside concentric annular spaces is analyzed. The material is assumed to behave as a generalized Newtonian liquid, with a modified Herschel–Bulkley viscosity function. The governing equations are solved numerically via a finite volume method. Two different thermal boundary conditions at the inner wall are considered, namely, uniform wall heat flux and uniform wall temperature. The outer wall is considered to be adiabatic. The effect of yield stress and power-law exponent on the Nusselt number is investigated. It is shown that the entrance length decreases as the material behavior departs from Newtonian. Also, it is observed that the effect of rheological parameters on the inner-wall Nusselt number is rather small.

Keywords: Forced convection; Viscoplastic materials; Annulus; Herschel–Bulkley materials

1. Introduction

The flow of viscoplastic materials is present in a large number of industrial processes. These include sterilization or packaging processes of foods, pharmaceutic products, cosmetics and lubricants, the drilling process of oil wells, and the extrusion of ceramic catalyst supports, to name a few. In these processes, heat transfer information is sometimes needed to predict temperature levels, which either must or cannot be achieved for successful results. In other applications, heat transfer rates are to be controlled to cause a desired rheology of the flowing material.

An interesting example is the drilling process of petroleum wells. To accomplish a number of functions, the drilling mud flows down through the column and then up through the annular space between the column and the rock formation. The drilling fluid must have the appropriate properties to ensure the success of a drilling operation. It should have the correct density to provide the pressure needed for well integrity and for avoiding premature production of hydrocarbons. As far as the fluid rheology is concerned, a highly shear-thinning behavior is desired, to ensure the transport of the drilled cuttings at reasonably low pumping power. However, in order to assure the correct properties of the drilling fluid during the process, especially the rheological ones which are typically strong functions of temperature, the heat transfer rates occurring during the process must be accessible a priori.

Escudier et al. (2002) analyzed the fully developed laminar flow of a generalized Newtonian fluid through annuli, with a power-law viscosity function. The effects of eccentricity and inner-cylinder rotation were studied. An extensive literature review about laminar flows of non-Newtonian fluids through annular spaces was also presented. Round and Yu (1993) analyzed the developing flows of Herschel–Bulkley fluids through concentric annuli. The effects of rheological parameters on velocity and pressure profiles were investigated.

Numerous articles about heat transfer during axisymmetric flows of non-Newtonian fluids can be found in the literature. Several authors (Bird et al., 1987; Irvine and Karni, 1987; Joshi and Bergles, 1980a,b; Scirocco et al.,

* Corresponding author. Tel.: +55-21-529-9333; fax: +55-21-294-9148.
E-mail address: pmendes@mec.puc-rio.br (P.R. Souza Mendes).

0142-727X/$ - see front matter © 2003 Elsevier Inc. All rights reserved.
doi:10.1016/S0142-727X(03)00066-3

Nomenclature

c_p	specific heat at constant pressure (J/kg K)
D_H	hydraulic diameter (m), $D_H = 2(R_o - R_i)$
f	Darcy friction factor
K	consistency index (Pa s^n)
n	power-law exponent
Nu	Nusselt number, $Nu \equiv hD_H/\kappa$
p	pressure (Pa)
P'	dimensionless pressure, $P' \equiv p/\tau_c$
Pe	Péclet number, $Pe \equiv \rho c_p \bar{u} D_H/\kappa$
q_w	inner wall heat flux (W/m^2)
r'	dimensionless radial coordinate, $r' = r/\delta$
R_i	inner radius (m)
R_o	outer radius (m)
Re	Reynolds number, $Re \equiv \rho \bar{u} D_H/\eta_c$
T	temperature (K)
T_b	bulk temperature (K)
T_{in}	inlet fluid temperature (K)
T_w	inner wall temperature (K)
u'	dimensionless axial velocity, $u' = u/\delta\dot{\gamma}_c$
$\bar{u}$	mean velocity vector (m/s)
$\bar{u}'$	mean velocity vector (m/s)
v'	dimensionless radial velocity, $v' = v/\delta\dot{\gamma}_c$
$\mathbf{v}$	velocity vector (m/s)
x'	dimensionless axial coordinate, $x' = x/\delta$

Greeks

α	fluid thermal diffusivity (m^2/s)
δ	hydraulic radius (m), $\delta = R_o - R_i$
$\dot{\gamma}_c$	characteristic shear rate (1/s), $\dot{\gamma}_c \equiv ((\tau_c - \tau_o)/K)^{1/n}$
$\dot{\boldsymbol{\gamma}}$	rate-of-deformation tensor (1/s), $\dot{\boldsymbol{\gamma}} \equiv \text{grad}\mathbf{v} + (\text{grad}\mathbf{v})^T$
$\dot{\gamma}$	magnitude of the rate-of-deformation tensor (1/s), $\dot{\gamma} \equiv \sqrt{(1/2)\text{tr}\dot{\boldsymbol{\gamma}}^2}$
Γ	auxiliary constant, $\Gamma \equiv (2\omega q_w)/(\kappa R_o(1-\omega^2))$
η	viscosity function (Pa s)
η_c	characteristic viscosity (Pa s)
η'	dimensionless viscosity function, $\eta' = \eta/\eta_c$
κ	fluid thermal conductivity (W/m K)
λ	dimensionless radial coordinate where $\tau' = 0$
λ_1	dimensionless radial coordinate where $\tau' = -\tau'_0$
λ_2	dimensionless radial coordinate where $\tau' = \tau'_0$
ω	radius ratio, $\omega = R_i/R_o$
θ	dimensionless temperature for the uniform heat flux boundary condition, $\theta \equiv (T - T_{in})/(q_w D_H/\kappa)$ and for the uniform temperature boundary condition, $\theta \equiv (T - T_w)/(T_{in} - T_w)$
θ_b	dimensionless bulk temperature
θ_w	dimensionless inner wall temperature
ρ	fluid density (kg/m^3)
τ_c	characteristic shear stress (Pa), $\tau_c = (-\text{d}p/\text{d}x)D_H/4$
$\boldsymbol{\tau}$	extra-stress tensor (Pa), $\boldsymbol{\tau} \equiv \mathbf{T} + P\mathbf{1}$
τ	magnitude of the extra-stress tensor (Pa), $\tau \equiv \sqrt{(1/2)\text{tr}\boldsymbol{\tau}^2}$
τ_0	yield stress (Pa)
τ'_0	dimensionless yield stress, $\tau' = \tau/\tau_c$
τ_{rx}	rx component of shear stress (Pa)
τ'_{R_i}	dimensionless shear stress at inner wall
τ'_{R_o}	dimensionless shear stress at outer wall
τ_s	representative value of shear stress (Pa), $\tau_s = (R_o\lvert\tau_{R_o}\rvert + R_i\lvert\tau_{R_i}\rvert)/(R_o + R_i)$
τ_w	wall shear stress (Pa), $\tau_w = 8\mu\bar{u}/D$

1985) analyzed the heat transfer problem in flows of power-law fluids through tubes and proposed correlations for the Nusselt number.

Manglik and Fang (2002) investigated numerically heat transfer to a power-law fluid flowing through an eccentric annular space. The outer wall was adiabatic, and two boundary conditions at the inner wall are analyzed: uniform heat flux and uniform temperature. Numerical solutions for the velocity and temperature fields are presented and discussed, for both shear-thinning and shear-thickening fluids. They found that the power-law index does not change significantly the Nusselt number for concentric annular spaces.

Vradis et al. (1992) analyzed numerically the heat transfer problem for developing flows of constant-property Bingham materials through tubes. They focused on the case of simultaneous velocity and temperature development. Nouar et al. (1994) reported an experimental and theoretical heat transfer study for Herschel–Bulkley materials inside tubes, for fully developed velocity profiles and developing temperature field. The impact of temperature-dependent rheological properties on the velocity profiles and on the Nusselt number was also discussed. Nouar et al. (1995) also analyzed numerically the heat transfer to Herschel–Bulkley materials flowing through tubes considering temperature-dependent consistency index and simultaneous velocity and temperature development, and neglecting axial diffusion of heat. Correlations for the local Nusselt number and pressure gradient were proposed. Soares et al. (1999) studied the developing flow of Herschel–Bulkley materials inside tubes, for constant and temperature-dependent properties, taking axial diffusion into account. Among other results, they observed that the temperature-dependent properties do not affect qualitatively pressure drop or the Nusselt number.

Also, it was shown that axial diffusion is important near the tube inlet.

Heat transfer to viscoplastic materials through annular flows was investigated experimentally by Naimi et al. (1990). In their work, the inner cylinder was able to rotate, and secondary flows appear due to rotation. The heat transfer coefficient was obtained as a function of the axial coordinate and angular velocity of the inner cylinder. Soares et al. (1998) studied heat transfer in a fully developed flow of Herschel–Bulkley materials through annular spaces, with insulated outer wall and uniform heat flux at the inner wall. For that case it was observed that the Nusselt number depends rather little on the rheological properties. Nascimento et al. (2002) analyzed the developing flow of Bingham fluids through concentric annuli using a finite transform technique. The results obtained showed that the Nusselt number increases with the dimensionless yield stress along the thermal entry region, but is nearly insensitive to it at the fully developed region.

In the present work, heat transfer to Herschel–Bulkley materials in laminar axial flow through concentric annular spaces is analyzed numerically. The region of simultaneous hydrodynamic and thermal development is considered. The effects of rheological parameters on the Nusselt number are investigated for two different thermal boundary conditions at the inner wall. The outer wall is assumed to be adiabatic.

2. Analysis

The flow under study is steady and axisymmetric. The outer and inner radii of the concentric annulus are R_o and R_i, respectively. In order to model the viscoplastic behavior of the fluid, the generalized Newtonian liquid constitutive equation is used, where $\boldsymbol{\tau} = \eta\dot{\boldsymbol{\gamma}}$. $\boldsymbol{\tau}$ is the extra-stress tensor and $\dot{\boldsymbol{\gamma}} \equiv \mathrm{grad}\mathbf{v} + (\mathrm{grad}\mathbf{v})^{\mathrm{T}}$ is the rate-of-deformation tensor, where $\mathbf{v}$ is the velocity vector. The viscosity function for yield-stress materials is generally well represented by the Herschel–Bulkley equation (Bird et al., 1987):

$$\eta = \begin{cases} \frac{\tau_0}{\dot{\gamma}} + K\dot{\gamma}^{n-1}, & \text{if } \tau > \tau_o \\ \infty, & \text{otherwise} \end{cases} \tag{1}$$

In Eq. (1), τ_o is the yield stress of the material, $\tau \equiv \sqrt{(1/2)\mathrm{tr}\boldsymbol{\tau}^2}$ is a measure of the magnitude of $\boldsymbol{\tau}$, $\dot{\gamma} \equiv \sqrt{(1/2)\mathrm{tr}\dot{\boldsymbol{\gamma}}^2}$ is a measure of the magnitude of $\dot{\boldsymbol{\gamma}}$, K is the consistency index, and n is the power-law exponent. These rheological parameters that appear in Eq. (1) are assumed to be independent of temperature as a first approximation.

In order to make the conservation equations dimensionless, a few characteristic quantities are now introduced. Firstly, the characteristic length is chosen to be the gap of the annular space:

$$\delta = \frac{D_H}{2} = R_o - R_i \tag{2}$$

where $D_H = 2(R_o - R_i)$ is the hydraulic diameter for annuli.

The characteristic shear stress, τ_c, shear rate, $\dot{\gamma}_c$, and viscosity, η_c, are chosen to be the values of these quantities that would occur at the wall of a tube of diameter D_H for fully developed flow conditions:

$$\tau_c \equiv -\frac{\mathrm{d}p}{\mathrm{d}x}\frac{D_H}{4} = -\frac{\mathrm{d}p}{\mathrm{d}x}\frac{R_o}{2}(1-\omega) \tag{3}$$

$\omega \equiv R_i/R_o$ is the radius ratio.

$$\dot{\gamma}_c \equiv \left[\frac{\tau_c - \tau_o}{K}\right]^{\frac{1}{n}} \tag{4}$$

$$\eta_c \equiv \eta(\dot{\gamma}_c) = \frac{\tau_c}{\dot{\gamma}_c} \tag{5}$$

The dimensionless mass conservation equation for this axisymmetric flow is given by:

$$\frac{1}{r'}\frac{\partial}{\partial r'}(r'v') + \frac{\partial}{\partial x'}(u') = 0 \tag{6}$$

The dimensionless radial and axial coordinates that appear in Eq. (6) are defined respectively as $r' = r/\delta$ and $x' = x/\delta$. The dimensionless axial and radial velocity components are respectively defined as $u' = u/\delta\dot{\gamma}_c$ and $v' = v/\delta\dot{\gamma}_c$.

Momentum conservation in axial and radial directions, respectively, is assured when the following dimensionless equations are satisfied:

$$\begin{aligned}\frac{1}{r'}\frac{\partial}{\partial r'}(r'v'u') + \frac{\partial}{\partial x'}(u'u') &= \frac{2\bar{u}'}{Re}\left[\frac{1}{r'}\frac{\partial}{\partial r'}\left(\eta' r'\frac{\partial v_x'}{\partial r'}\right) + \frac{\partial}{\partial x'}\left(\eta'\frac{\partial u'}{\partial x'}\right)\right. \\ &\left. + \frac{\partial\eta'}{\partial r'}\frac{\partial v'}{\partial x'} + \frac{\partial\eta'}{\partial x'}\frac{\partial u'}{\partial x'}\right] - \frac{\partial P'}{\partial x'}\end{aligned} \tag{7}$$

$$\begin{aligned}\frac{1}{r'}\frac{\partial}{\partial r'}(r'v'v') + \frac{\partial}{\partial x'}(v'u') &= \frac{2\bar{u}'}{Re}\left[\frac{1}{r'}\frac{\partial}{\partial r'}\left(\eta' r'\frac{\partial v'}{\partial r'}\right) + \frac{\partial\eta'}{\partial r'}\frac{\partial v'}{\partial r'}\right. \\ &\left. + \frac{\partial\eta'}{\partial x'}\frac{\partial u'}{\partial r'} - \eta'\frac{v'}{r'^2}\right] - \frac{\partial P'}{\partial r'}\end{aligned} \tag{8}$$

In the above expressions, $\eta' = \eta/\eta_c$ is the dimensionless viscosity, $P' = p/\tau_c$ is the dimensionless pressure and $Re \equiv \rho\bar{u}D_H/\eta_c$ is the Reynolds number.

The dimensionless energy equation is given by:

$$\begin{aligned}\frac{1}{r'}\frac{\partial}{\partial r'}(r'v'\theta) + \frac{\partial}{\partial x'}(u'\theta) &= \frac{2\bar{u}'}{Pe}\left[\frac{1}{r'}\frac{\partial}{\partial r'}\left(r'\frac{\partial\theta}{\partial r'}\right) + \frac{\partial}{\partial x'}\left(\frac{\partial\theta}{\partial x'}\right)\right]\end{aligned} \tag{9}$$

In this equation θ is the dimensionless temperature, to be defined shortly, and $Pe \equiv \rho c_p\bar{u}D_H/\kappa$ is the Péclet

number, where ρ is the mass density, c_p the specific heat at constant pressure, $\bar{u}$ the mean axial velocity, and κ the thermal conductivity.

The boundary conditions are the no slip at the solid walls, uniform velocity and temperature profiles at the inlet and developed flow at the outlet. Two thermal boundary conditions are investigated for the inner wall: uniform wall heat flux (q_w = constant) and uniform wall temperature (T_w = constant). The outer wall is assumed to be perfectly insulated ($q_w = 0$). For the case of uniform wall heat flux boundary condition, θ is defined as:

$$\theta \equiv \frac{T - T_{in}}{q_w D_H/\kappa}$$

where q_w is the heat flux at the inner wall and T_{in} is the inlet fluid temperature. For cases pertaining to the uniform wall temperature boundary condition, θ is given by:

$$\theta \equiv \frac{T - T_w}{T_{in} - T_w}$$

where T_w is the inner wall temperature.

2.1. Nusselt number

For the case of uniform heat flux at the inner wall, the Nusselt number can be expressed as:

$$Nu \equiv \frac{hD_H}{\kappa} = \frac{1}{\theta_w(x') - \theta_b(x')} \tag{10}$$

where h is the heat transfer coefficient and $\theta_b = (T_b - T_{in})/(q_w D_H/\kappa)$ is the dimensionless bulk temperature. The bulk temperature, T_b, is given by:

$$T_b \equiv \frac{\int_{R_i}^{R_o} uTr\,dr}{\int_{R_i}^{R_o} ur\,dr} \tag{11}$$

For the case of uniform inner wall temperature, the Nusselt number is given by:

$$Nu \equiv \frac{hD_H}{\kappa} = \frac{-2\frac{\partial\theta}{\partial r'}\left(\frac{\omega}{1-\omega}, x'\right)}{\theta_b(x')} \tag{12}$$

For this situation, $\theta_b = (T_b - T_w)/(T_{in} - T_w)$.

2.2. Range of yield stress

In this section, we present a discussion regarding the range of yield stress values which are consistent with the above formulation. As we will explain, for the case of the axial flow of viscoplastic materials through annuli, values of $\tau_o' \equiv \tau_o/\tau_c$ within a narrow range are expected to be related to continuous, non-zero velocity fields. Clearly, this information is needed prior to attempting numerical solutions. The existence of this restricting range is not obvious a priori, and we now show how it is determined.

We start this analysis with the axial-direction momentum equation, which, for fully developed flow, can be written as follows:

$$\frac{1}{r}\frac{d}{dr}(r\tau_{rx}) = \frac{dp}{dx} \tag{13}$$

Now we notice that the shear stress values at both the outer and inner walls must have signs such that both produce shear forces which oppose to the flow. Therefore, it is clear that $\tau_{rx}(R_o) = \tau_c < 0$ and $\tau_{rx}(R_i) = \tau_{R_i} > 0$. Consequently, there is a radial position, $r = \lambda R_o$, where the rx shear stress component vanishes, i.e., $\tau_{rx}(\lambda R_o) = 0$. Eq. (13) is then integrated, and the constant of integration is eliminated in favor of λ. The dimensionless form of the solution is

$$\tau' = \frac{\lambda^2}{(1-\omega)^2 r'} - r' \tag{14}$$

where $\tau' = \tau_{rx}/\tau_c$ is the dimensionless shear stress. Eq. (14) can be evaluated at the outer wall ($r' = 1/(1-\omega)$) and at the inner wall ($r' = \omega/(1-\omega)$), yielding the following expressions for the two wall shear stresses:

$$\tau'_{R_o} = \frac{\lambda^2 - 1}{1-\omega}; \quad \tau'_{R_i} = \frac{\lambda^2 - \omega^2}{\omega(1-\omega)} \tag{15}$$

From Eq. (15) it is seen that, in general $|\tau'_{R_i}|$ may be larger, equal or smaller than $|\tau'_{R_o}|$, depending upon the value of λ. Actually, λ depends on the material behavior. For Newtonian fluids, for example, $\lambda = \sqrt{-(1-\omega^2)/2\ln\omega}$, and for a viscoplastic material it depends on the dimensionless yield stress τ_o' (Fredrickson and Bird, 1958).

We now introduce the dimensionless parameters λ_1 and λ_2, such that $\tau'(\lambda_1 R_o) = -\tau_o'$ and $\tau'(\lambda_2 R_o) = \tau_o'$. It is worth noting that, by definition, $\lambda_1 > \lambda_2$.

If we now evaluate Eq. (14) at $r' = \lambda_1/(1-\omega)$ (where $\tau' = -\tau_0'$) and at $r' = \lambda_2/(1-\omega)$ (where $\tau' = \tau_0'$) we obtain the following expressions for λ_1 and λ_2:

$$\lambda_1 = \frac{(1-\omega)\tau_0' + \sqrt{(1-\omega)^2\tau_0'^2 + 4\lambda^2}}{2} \tag{16}$$

$$\lambda_2 = \frac{-(1-\omega)\tau_0' + \sqrt{(1-\omega)^2\tau_0'^2 + 4\lambda^2}}{2} \tag{17}$$

Eqs. (16) and (17) are combined to give the following expression for τ_0':

$$\tau_0' = \frac{\lambda_1 - \lambda_2}{1-\omega} \tag{18}$$

This equation indicates that τ_0' represents the dimensionless size of the plug flow region. We also note that when both $\lambda_1 < 1$ and $\lambda_2 > \omega$ then flow will occur, and the dimensionless yield stress satisfies the following restriction:

$$\tau_0' < 1 \tag{19}$$

In summary, it can be concluded that, when there is flow, then the characteristic stress is larger than the material yield stress. Because we cannot determine λ before specifying the constitutive behavior of the flowing material, the above analysis does not allow us to conclude the reverse, namely, that whenever $\tau_0' < 1$ then necessarily flow occurs. We cannot affirm either that there will be no flow when $\tau_0' > 1$.

Actually, the discussion above indicates that there are in principle four possible situations for viscoplastic materials, namely:

1. the pressure gradient, $|\mathrm{d}p/\mathrm{d}x|$, is not strong enough to generate a stress profile $\tau(r)$, which magnitude of its maximum exceeds the yield stress, τ_0. In this case there is no flow (Case 1, Fig. 1).
2. $|\mathrm{d}p/\mathrm{d}x|$ generates a stress profile which values at the inner and outer walls, τ_{R_i} and τ_{R_o} respectively, are both, in magnitude, larger than τ_0. In such case there is flow, and a plug flow region ($\dot{\gamma} = 0$) appears, where the stress is below the yield stress (Case 2, Fig. 1).
3. $|\mathrm{d}p/\mathrm{d}x|$ and λ are such that $|\tau_{R_\mathrm{i}}| < \tau_0 < |\tau_{R_\mathrm{o}}|$. In this case there will be flow in the region close to the outer wall only, where $|\tau| > \tau_0$. Everywhere else in the annular space, there is no flow. This situation is only possible if there is a discontinuity in the velocity profile (fracture or slip inner surface) at the radial position where $|\tau| = \tau_0$ (Case 3, Fig. 1).
4. $|\mathrm{d}p/\mathrm{d}x|$ and λ are such that $|\tau_{R_\mathrm{o}}| < \tau_0 < |\tau_{R_\mathrm{i}}|$. This case is analogous to the previous one, with the discontinuity occurring in the vicinity of the inner wall (Case 4, Fig. 1).

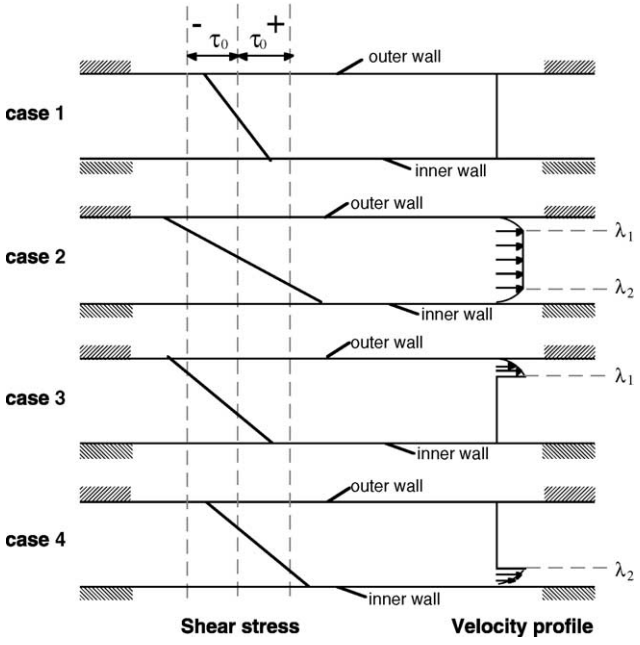

Fig. 1. Possible types of axial flow of viscoplastic materials through annular spaces.

While it is quite easy to accept the existence of Cases 1 and 2, the same cannot be said with respect to Cases 3 and 4, due to the seemingly non-realistic discontinuities in the axial velocity profile. However, it is worth emphasizing that Cases 3 and 4 are in agreement with the conservation principles and therefore cannot be discarded a priori.

On the other hand, the solution presented by Fredrickson and Bird (1958) for Bingham plastics assumes a priori the situation depicted in Case 2. One quite interesting feature of this solution is that both wall shear stresses become simultaneously equal to the material yield stress as the no-flow situation is approached. In other words, as $\lambda_1 \to 1$, it also occurs that $\lambda_2 \to \omega$. For this limiting no-flow situation, clearly $\tau_\mathrm{o}' = 1$, and $\lambda = \sqrt{\omega}$. Therefore, there is a transition from Cases 2 to 1 as the pressure gradient is decreased, which rules out the possibility of occurrence of either Cases 3 or 4.

The above facts are true for Bingham plastics, as it can be inferred from the solution of Fredrickson and Bird (1958). Therefore, they constitute no basis for concluding that the same facts are to be observed for other viscoplastic materials, although they do reinforce the suspicion that Cases 3 and 4 are not attainable for other viscoplastic materials either.

As it will be shown in Section 4, we sought for numerical solutions within the range dictated by Eq. (19) only, and all the results obtained were found to pertain to Case 2.

2.3. Using fRe for checking the accuracy of numerical results

For the fully-developed flow of Newtonian fluids of viscosity μ through tubes of diameter D, the Reynolds number $Re = \rho\bar{u}D/\mu = 8\rho\bar{u}^2/\mu(8\bar{u}/D)$ is the ratio of a representative inertial force to a representative viscous force. The term $8\bar{u}/D$ is the shear rate at the tube wall for a fully developed flow of a Newtonian fluid, and hence the corresponding wall shear stress is $\tau_\mathrm{w} = \mu(8\bar{u}/D)$. Accordingly, for internal fully-developed flows of non-Newtonian materials through other types of ducts, we can generalize the definition of Re as

$$Re = \frac{8\rho\bar{u}^2}{\tau_\mathrm{s}} \tag{20}$$

where τ_s is a representative value of shear stress that arises in an overall momentum balance at the fully developed region. For the annular space, such momentum balance yields:

$$-\frac{\mathrm{d}p}{\mathrm{d}x}\frac{D_\mathrm{H}}{4} \equiv \tau_\mathrm{s} = \frac{R_\mathrm{o}|\tau_{R_\mathrm{o}}| + R_\mathrm{i}|\tau_{R_\mathrm{i}}|}{R_\mathrm{o} + R_\mathrm{i}} \tag{21}$$

It is noted that τ_s is a good choice for characteristic stress, as we did in the present work. The friction factor f is usually defined as

$$f = \frac{-\frac{dp}{dx} D_H}{\frac{1}{2}\rho \bar{u}^2} \tag{22}$$

Therefore, making use of the definition of Reynolds number given by Eq. (20), the product between the friction factor and the Reynolds number, fRe, becomes:

$$fRe = \frac{-16\frac{dp}{dx} D_H}{\tau_s} \tag{23}$$

It is seen that the product fRe can be conveniently interpreted as the ratio of a characteristic pressure drop to the shear stress that opposes to it. Moreover, if it is defined as explained above, it is always true that

$$fRe = 64 \tag{24}$$

regardless the rheological behavior and the duct geometry.

Of course the result of Eq. (24) alone is useless for determining the flow rate as a function of pressure drop, because it is merely a manipulation of the momentum balance (Eq. (21)), adding no new information to it. For laminar flow of Newtonian fluids through tubes, the fact that $fRe = 64$ can be used in this connection just because we also know a priori, from the analytical solution, how to relate τ_s to the flow rate, namely, $\tau_s = \mu(8\bar{u}/D)$. For flows of non-Newtonian materials through tubes or other types of ducts, in general this information is not available, because we need the velocity field to evaluate the shear rate at the wall(s), which is needed for determining τ_s.

Nevertheless, Eq. (24) can be quite useful in these cases while obtaining numerical solutions, during the process of selecting an appropriate mesh for the problem. The numerically obtained shear rates can be employed to evaluate τ_s (through the constitutive equation) and subsequently fRe. Meshes that do not give values of fRe close enough to 64 should not be used. This procedure was employed in the present work.

2.4. Modified bi-viscosity model

The Herschel–Bulkley viscosity function given by Eq. (1) is not easy to handle numerically. One of its inconveniences is that the field of second invariant of extra-stress, τ, must be evaluated at each iteration. However, its main problem is its inconsistency with certain types of flows due to the imposition of rigid-body motion in the regions where $\tau < \tau_o$ (Lipscomb and Denn, 1984; Al Khatib and Wilson, 2001).

For example, along the entrance region of a tube flow, the centerline velocity must increase with the axial coordinate, to satisfy continuity. This implies extensional deformation of all material elements located at the centerline in the entrance region. However, at the centerline the shear stress is null due to symmetry, and τ is expected to decrease monotonically to zero with the axial coordinate, as the flow develops. Therefore, there will be a portion of the centerline, within the entrance region and just upstream the fully-developed flow region, along which $\tau < \tau_o$ and hence where no deformation is allowed. This physical inconsistency should lead to non-convergence in any attempt to use the Herschel–Bulkley viscosity function in numerical formulations for flows with characteristics similar to the one mentioned in the just discussed example.

To remedy this, two types of alternative viscosity functions were proposed for Bingham materials, namely, the bi-viscosity model (Lipscomb and Denn, 1984; Gartling and Phan-Thien, 1984; O'Donovan and Tanner, 1984), and the Papanastasiou model (Papanastasiou, 1987). Both modifications have been used successfully in numerical simulations of different complex flows (Ellwood et al., 1990; Abdali et al., 1992; Beverly and Tanner, 1992; Wilson, 1993; Wilson and Taylor, 1996; Piau, 1996). The idea is to impose a very high viscosity in the regions where $\tau < \tau_o$. This replaces the rigid-body motion with a rather slow deformation, thus removing the inconsistency discussed above. The bi-viscosity model can be easily extended to Herschel–Bulkley materials, and was used in this work. The resulting expression for the viscosity function is given by:

$$\eta' = \begin{cases} \frac{\tau'_o}{\dot{\gamma}'} + (1-\tau'_o)\dot{\gamma}'^{n-1}, & \text{if } \dot{\gamma}' > \dot{\gamma}'_{small} \\ \eta'_{large}, & \text{otherwise} \end{cases} \tag{25}$$

In the above equations, $\dot{\gamma}' \equiv \dot{\gamma}/\dot{\gamma}_c$ is the dimensionless shear rate, and η'_{large} is a large dimensionless number. Beverly and Tanner (1992) recommend $\eta'_{large} = 1000$. Accordingly, $\dot{\gamma}'_{small} = \tau'_o/[1000 - (1-\tau'_o)\dot{\gamma}'^{n-1}_{small}] \simeq \tau'_o/1000$.

3. Numerical method

The governing equations presented above were discretized with the aid of the finite volume method described by Patankar (1980). Staggered velocity components were employed to avoid unrealistic pressure fields. The SIMPLE algorithm (Patankar, 1980) was used, in order to handle the coupling between pressure and velocity. The resulting system of algebraic equations was solved via the line-by-line TDMA (Patankar, 1980) in conjunction with the block correction algorithm (Settari and Aziz, 1973) to increase the convergence rate.

The length of the computational domain was held fixed at a value of $L/\delta = 40$. A non-uniform mesh was used, with an increasing concentration of grid points toward the duct inlet. Extensive mesh tests were performed in order to choose an adequate mesh, and one

with 102 grid points in the axial direction and 62 grid points in the radial direction were found to yield good results. The error obtained for the fully-developed value of the product *fRe* for a Newtonian fluid and $\delta/R_o = 0.5$ was 0.5%.

For the thermal boundary conditions of adiabatic inner wall and uniform temperature at the outer wall, the error obtained for the Newtonian Nusselt number, Nu_{Dh}, was 1.6%. For the viscoplastic material and $Re = 50$, $Pe = 100$, $\tau_0' = 0, 17$ and $n = 0, 5$, *fRe* and *Nu* values were obtained with different meshes. The difference between results obtained with the mesh used and the ones obtained with a 80×50 mesh was of 0.4% for *fRe* and 0.2% for *Nu*.

The numerical solution was also compared with analytical solutions some specific flows of non-Newtonian materials. The velocity field obtained numerically was in excellent agreement with the exact solution obtained by Fredrickson and Bird (1958) for a Bingham plastic. The velocity field for the flow of a viscoplastic material through an annular space with radius ratio tending to unity compared very well with the exact solution for the flow of Herschel–Bulkley material with same rheological parameters through a parallel plate channel. Finally, we compared the numerical velocity field with the experimental data obtained by Naimi et al. (1990). A good agreement was obtained, except for a small difference observed near the walls, which was probably due to our difficulty in accessing the exact values of rheological parameters of the fluid used in the experiments.

4. Results and discussion

Results for some representative combinations of the governing parameters are now presented and discussed. Firstly, typical dimensionless axial velocity profiles for the fully-developed region are shown in Figs. 2 and 3. It is observed that lower power-law indexes and larger yield stresses cause wider plug flow regions, as expected. Fig. 4 shows the dimensionless velocity profile for different axial positions. It can be noted that for $x/\delta = 1.624$ the flow is already fully developed for the case shown.

4.1. Uniform wall heat flux

Dimensionless temperature profiles for the thermal boundary condition of uniform heat flux at the inner wall for fully-developed flow are shown in Figs. 5 and 6, for different combinations of the rheological parameters. Despite the velocity profile variation, it can be noted that the dimensionless temperature is almost invariant with both τ_o' and n. The dimensionless temperature profile along the developing region is shown in Fig. 7 for three different axial positions.

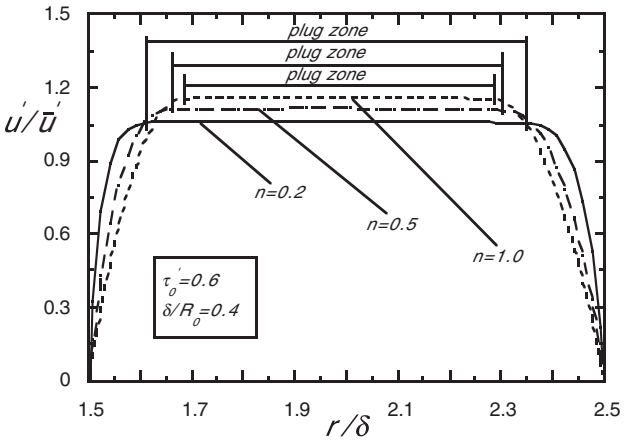

Fig. 2. Fully-developed velocity profile for different values of n.

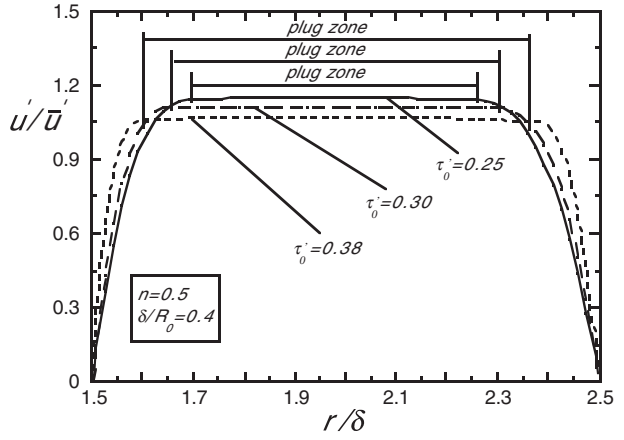

Fig. 3. Fully-developed velocity profile for different values of τ_o'.

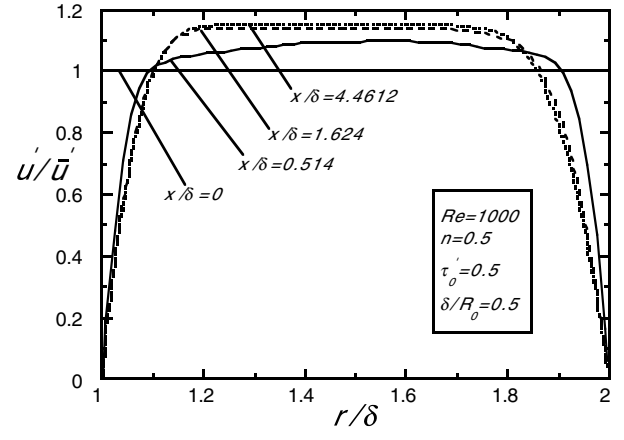

Fig. 4. Velocity profile variation with axial position.

The Nusselt number variation with geometrical, rheological and flow parameters are showed in Figs. 8–11. All the results presented were obtained considering axial diffusion. Soares et al. (1999) observed that the effect of

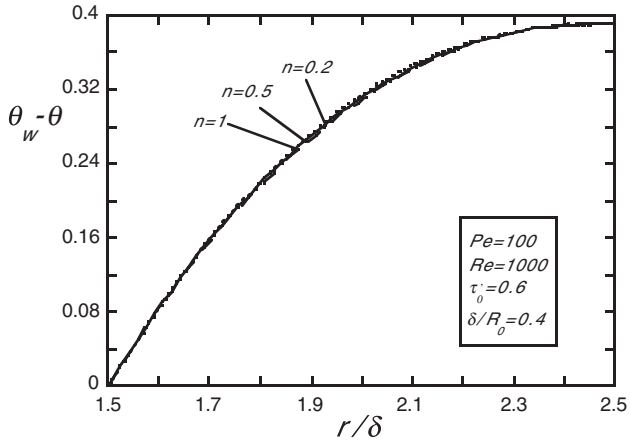

Fig. 5. Fully-developed temperature profile for different values of the power-law index, for uniform heat flux at the inner wall.

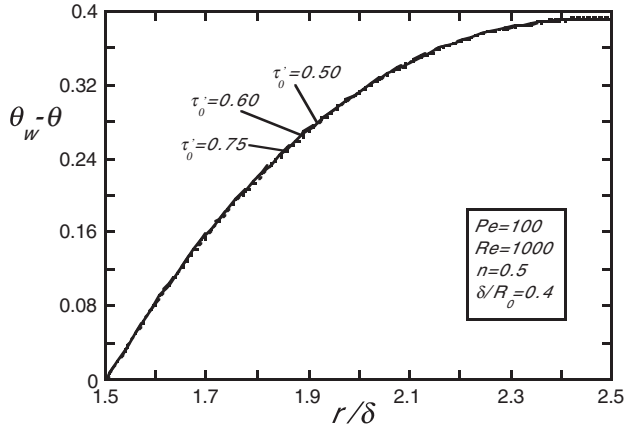

Fig. 6. Fully-developed temperature profile for different values of the dimensionless yield stress, for uniform heat flux at the inner wall.

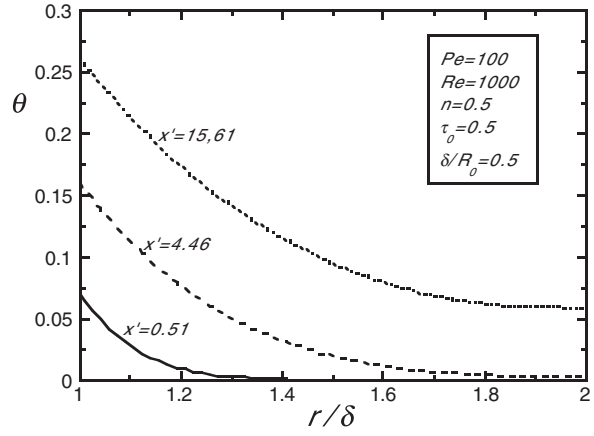

Fig. 7. Temperature profile for different axial positions, for uniform heat flux at the inner wall.

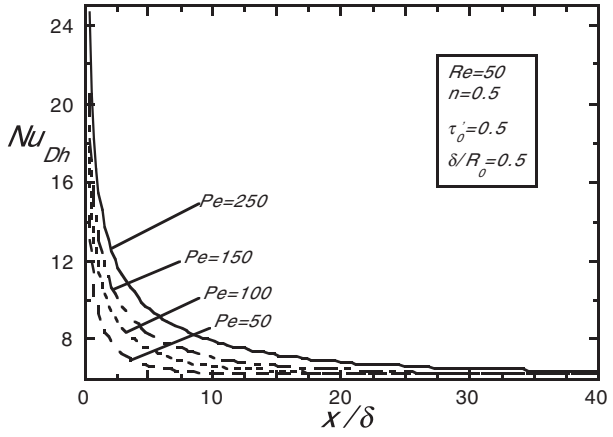

Fig. 8. Nusselt number variation with *Pe*, for uniform heat flux at the inner wall.

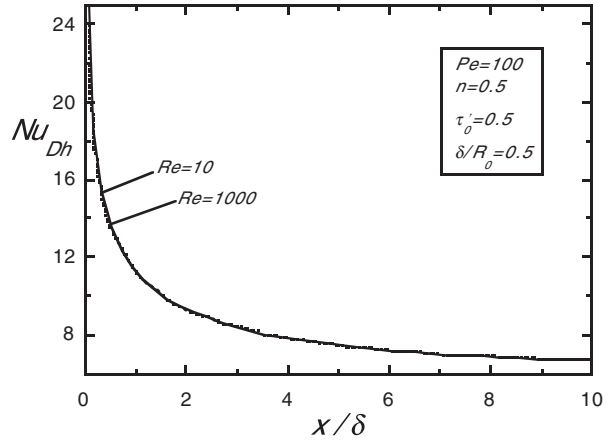

Fig. 9. Nusselt number variation with *Re*, for uniform heat flux at the inner wall.

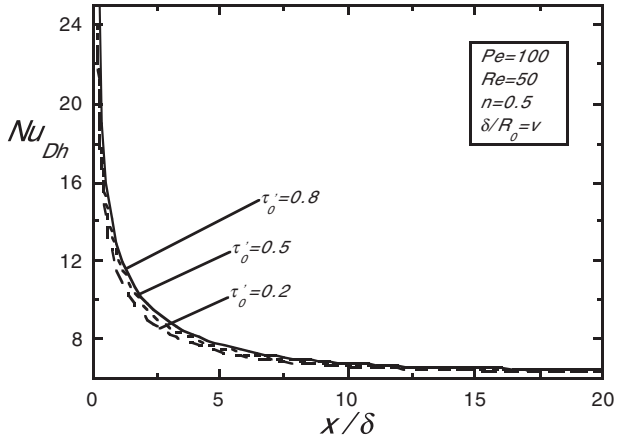

Fig. 10. Nusselt number variation with τ'_o, for uniform heat flux at the inner wall.

axial diffusion is not negligible and might have an important impact on heat transfer of viscoplastic fluid flows. Figs. 8 and 9 show the influence of the Péclet and Reynolds numbers on the Nusselt number, respectively.

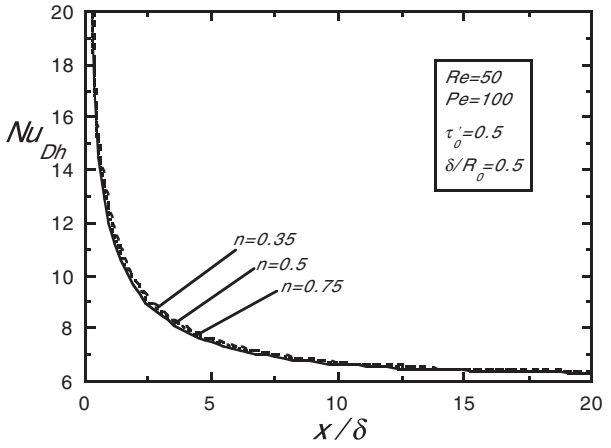

Fig. 11. Nusselt number variation with n, for uniform heat flux at the inner wall.

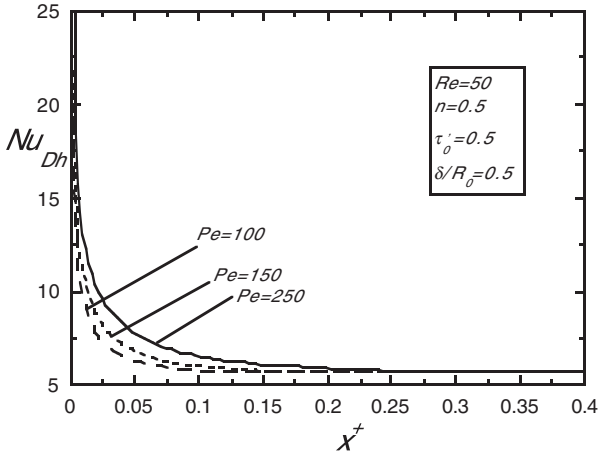

Fig. 13. Nusselt number variation with Pe, for uniform temperature at the inner wall.

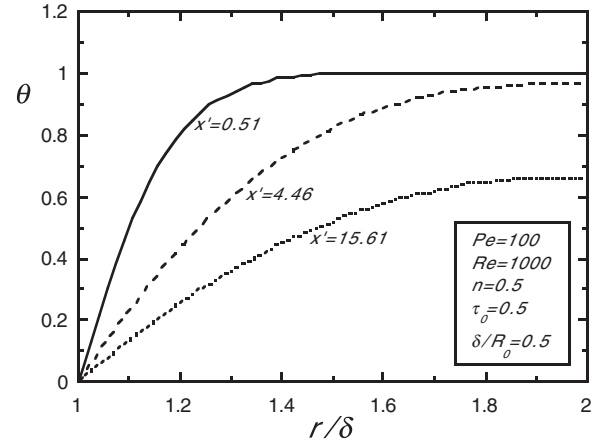

Fig. 12. Temperature profiles for different axial positions, for uniform temperature at the inner wall.

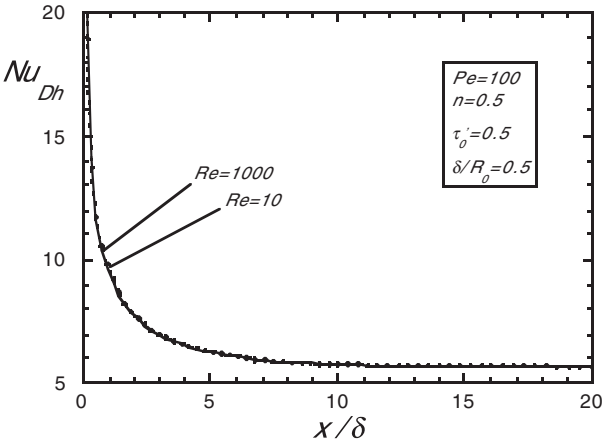

Fig. 14. Nusselt number variation with Re, for uniform temperature at the inner wall.

It can be noted that axial conduction is important only in the entrance region and its effect is to increase the Nusselt number. However, the Nusselt number is nearly independent of the Reynolds number.

The effects of rheological parameters on the Nusselt number are illustrated in Figs. 10 and 11. It can be observed that as the fluid behavior departs from Newtonian (increasing yield stress or decreasing power-law index), the Nusselt number increases. This fact is related to the wall velocity gradient, which increase with the widening of the plug-flow region. However, it can be noted that the sensitivity of the Nusselt number to these rheological parameters is rather small. This behavior is in contrast to what is observed for the flow through tubes, where Nu is a quite strong function of the rheological parameters (Soares et al., 1999). However, other researchers observed the same trend for flow through annuli with heated inner wall (Manglik and Fang, 2002; Nascimento et al., 2002).

4.2. Uniform wall temperature

Results for uniform temperature at the inner wall are now presented. Dimensionless temperature profiles along the developing region are shown in Fig. 12. The dimensionless temperature decreases with axial position, while the temperature gradient at the inner wall decreases, as expected.

Figs. 13–16 show the Nusselt number variation with flow and rheological parameters, for the uniform inner wall temperature boundary condition. It can be noted that the qualitative results are quite similar to the ones obtained for the cases of uniform wall heat flux. Fig. 13 shows that the Nusselt number increases with the Péclet number. However, as in the previous case, Nu is essentially unaffected by the Reynolds number.

Figs. 15 and 16 show the effect of the rheological parameters (n and τ_o'). These figures show that the Nusselt number increases as τ_o' increases, but increases

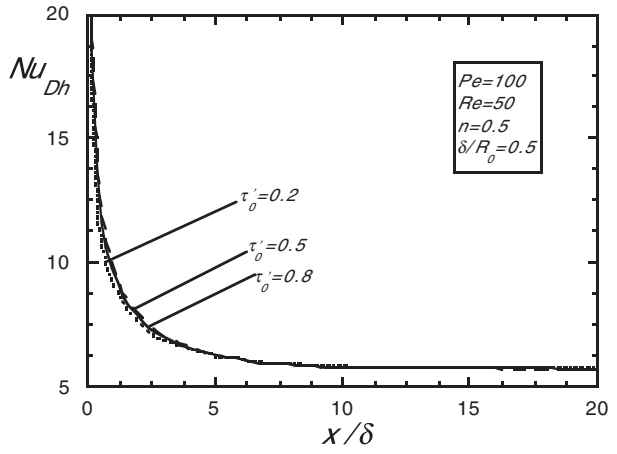

Fig. 15. Nusselt number variation with τ'_o, for uniform temperature at the inner wall.

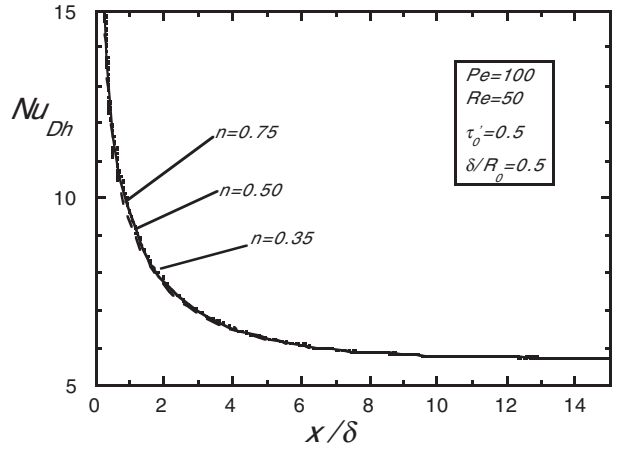

Fig. 16. Nusselt number variation with n, for uniform temperature at the inner wall.

as n decreases, as it was also observed for the other thermal boundary condition. However, the influence of the rheological parameters on Nu is again rather small.

4.3. Analysis for thermally developed plug flow

As it was discussed previously, the velocity gradients close to the walls increase as the fluid behavior departs from Newtonian. One limiting case of interest is the plug flow, i.e., the flow with an uniform axial velocity profile ($u(r) = U = \text{constant}$), which corresponds to $\tau'_o \to 1$ or to $n \to 0$.

For this limiting case, it is easy to obtain an analytical solution for the thermally developed situation of uniform heat flux at the inner wall. Because the numerical results for the Nusselt number turned out to be rather insensitive to the rheological parameters, in contrast to the results for tube flow available in the literature (Soares et al., 1999), an analytical solution is convenient not only to confirm this interesting and surprising trend, but also as a result that can be used in practical applications for all values of the rheological parameters.

For thermally developed plug flow, the energy conservation equation is written as

$$\frac{1}{r}\frac{\partial}{\mathrm{d}r}\left(r\frac{\partial T}{\partial r}\right) = \frac{U}{\alpha}\frac{\partial T}{\partial x} = \Gamma \tag{26}$$

where $\alpha = \kappa/\rho c_p$ is the thermal diffusivity, and Γ is a constant, namely

$$\Gamma \equiv \frac{2\omega q_w}{\kappa R_o(1-\omega^2)} \tag{27}$$

The temperature field is obtained upon integration of Eq. (26):

$$\theta = \theta_w - \left\{\frac{\omega}{4(1-\omega^2)(1-\omega)}\left(2\ln\left[\frac{1-\omega}{\omega}r'\right] - \left((1-\omega)^2 r'^2 - \omega^2\right)\right)\right\} \tag{28}$$

The Nusselt number can now be obtained as a function of radius ratio, upon integration of Eq. (28) along the cross-section:

$$Nu = \frac{1}{\theta_w - \theta_b} = \frac{8(\omega-1)(1-\omega^2)^2}{\omega[\omega^4 - 4\omega^2 + 4\ln(\omega) + 3]} \tag{29}$$

In Fig. 17 the Nusselt number is plotted as a function of the radius ratio as given by Eq. (29). The Nusselt number pertaining to flows of Newtonian fluids (Kakaç et al., 1987) is also plotted in this figure. The good agreement between the Newtonian and plug-flow Nusselt number values reinforces the the fact observed about the numerical results, namely, that the inner-wall Nusselt number is rather insensitive to the rheological behavior of the flowing fluid. The largest discrepancies that occur between the Newtonian and plug-flow Nusselt numbers (about 11%) occur for radius ratios near unity. For radius ratios below 0.5, the discrepancies are of the order of 2.5% only.

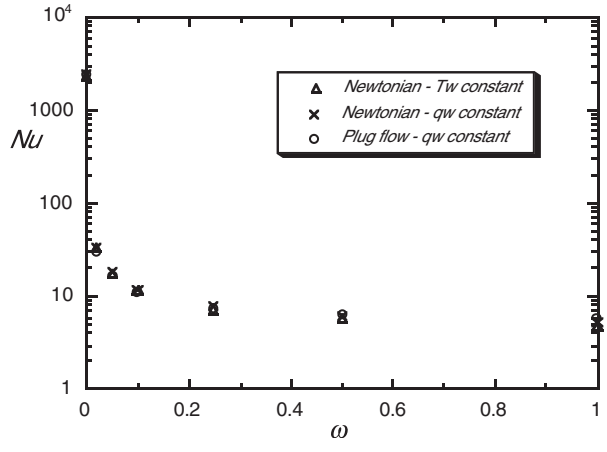

Fig. 17. Nusselt number variation with radius ratio, ω.

Finally, it is worth mentioning that, in the range of radius ratios below 0.5, the Newtonian Nusselt number found in the literature (Kakaç et al., 1987) is a little larger than the plug-flow Nusselt number as given by Eq. (29). This is quite surprising, because it seems physically reasonable to expect that the plug-flow Nusselt number is largest, as the trends observed in the numerical results indicate, and as it is the case for tube flow (Soares et al., 1999).

5. Conclusions

This paper presented a study of the heat transfer problem for the flow of Herschel–Bulkley materials through concentric annular spaces. Two temperature boundary conditions for the inner wall were analyzed: uniform heat flux and uniform temperature, while the outer wall assumed to be adiabatic.

The governing equations were solved numerically via a finite-volume technique. Results were presented in the form of velocity and temperature profiles, and Nusselt number as a function of rheological and geometrical parameters.

It was noted that Nusselt numbers are a little more sensitive to the parameters for the case of uniform heat flux. It was also observed that the higher is the velocity gradient at the wall, the higher will be the Nusselt number, as also observed for tube flow (Soares et al., 1999).

However, for all cases investigated the inner-wall Nusselt number is rather insensitive to the rheological behavior of the fluid. A comparison between Newtonian and plug-flow Nusselt numbers confirms such trend. This fact can be conveniently explored in practical applications, since the Newtonian Nusselt number available in the literature can be used regardless the rheological behavior of the fluid, with acceptable error for most engineering applications.

Acknowledgements

Financial support for the present research was partially provided by CENPES/PETROBRAS, CNPq, Faperj and MCT.

References

Abdali, S.S., Mitsoulis, E., Markatos, N.C., 1992. Entry and exit flows of Bingham fluids. J. Rheol. 36, 389.

Al Khatib, M.A.M., Wilson, S.D.R., 2001. The development of poiseulle flow of a yield-stress fluid. J. Non-Newton. Fluid Mech. 100, 1–8.

Beverly, C.R., Tanner, R.I., 1992. Numerical analysis of three-dimensional Bingham plastic flow. J. Non-Newton. Fluid Mech. 42, 85–115.

Bird, R.B., Armstrong, R.C., Hassager, O., 1987. In: Dynamics of Polymeric Liquids, vol. 1. Wiley.

Ellwood, K.R.J., Georgiou, G.C., Papanastasiou, C.J., Wilkes, J.O., 1990. Laminar jets of Bingham-plastic liquids. J. Rheol. 34, 787–812.

Escudier, M.P., Oliveira, P.J., Pinho, F.T., 2002. Fully developed laminar flow of purely viscous non-Newtonian liquids through annuli, including the effects of eccentricity and inner-cylinder rotation. Int. J. Heat Fluid Flow 23, 52–73.

Fredrickson, A.G., Bird, R.B., 1958. Non-Newtonian flow in annuli. Ind. Eng. Chem. 50, 347–352.

Gartling, D.K., Phan-Thien, N., 1984. A numerical simulation of a plastic fluid in s parallel-plate plastometer. J. Non-Newton. Fluid Mech. 14, 347–360.

Irvine Jr., T.F., Karni, J., 1987. Non-Newtonian fluid flow and heat transfer. In: Kakaç, S., Shah, R.K., Aung, W. (Eds.), Handbook of Single-phase Convective Heat Transfer. Wiley, pp. 20.1–20.57.

Joshi, S.D., Bergles, A.E., 1980a. Experimental study of laminar heat transfer to in-tube flow of non-Newtonian fluids. J. Heat Transfer 102, 397–401.

Joshi, S.D., Bergles, A.E., 1980b. Analytical study of laminar heat transfer to in-tube flow of non-Newtonian fluids, AICHE Symposium Series no. 199, vol. 76, pp. 270–281.

Kakaç, S., Shah, R.K., Aung, W., 1987. Handbook of Single-Phase Convective Heat Transfer. John Wiley & Sons.

Lipscomb, G.G., Denn, M.M., 1984. Flow of Bingham fluids in complex geometries. J. Non-Newton. Fluid Mech. 14, 337–346.

Manglik, R.M., Fang, P., 2002. Thermal processing of viscous non-Newtonian fluids in annular ducts: effects of power-law rheology, duct eccentricity, and thermal boundary conditions. Int. J. Heat Mass Transfer 45, 803–814.

Naimi, M., Devienne, R., Lebouche, M., 1990. Étude dynamique et thérmique de l'écoulement Couette-Taylor-Poiseuille; cas d'un fluide présentant en seuil d'écoulement. Int. J. Heat Mass Transfer 33, 381–391.

Nascimento, U.C.S., Macêdo, E.N., Quaresma, J.N.N., 2002. Thermal entry region analysis through the finite integral transform technique in laminar flow of Bingham fluids within concentric annular ducts. Int. J. Heat Mass Transfer 45, 923–929.

Nouar, C., Devienne, R., Lebouche, M., 1994. Convection thermique pour un fluide de Herschel–Bulkley dans la région d'entrée d'une conduite. Int. J. Heat Mass Transfer 37, 1–12.

Nouar, C., Lebouche, M., Devienne, R., Riou, C., 1995. Numerical analysis of the thermal convection for Herschel–Bulkley fluids. Int. J. Heat Fluid Flow 16, 223–232.

O'Donovan, E.J., Tanner, R.I., 1984. Numerical study of the Bingham squeeze film problem. J. Non-Newton. Fluid Mech. 15, 75–83.

Papanastasiou, T.C., 1987. Flows of materials with yield. J. Rheol. 31, 385–404.

Patankar, S.V., 1980. Numerical Heat Transfer and Fluid Flow. Hemisphere Publishing Co.

Piau, J.M., 1996. Flow of a yield stress fluid in a long domain. Application to flow on an inclined plane. J. Rheol. 40, 711–723.

Round, G.F., Yu, S., 1993. Entrance laminar flows of viscoplastic fluids in concentric annuli. Canadian J. Chem. Eng. 71, 642–645.

Scirocco, V., Devienne, R., Lebouche, M., 1985. Écoulement laminaire et transfert de chaleur pour un fluide pseudo-plastique dans la zone d'entrée d'un tube. Int J. Heat Mass Transfer 28, 91–99.

Settari, A., Aziz, K., 1973. A generalization of the additive correction methods for the iterative solution of matrix equations. SIAM J. Numer. Anal. 10, 506–521.

Soares, E.J., Naccache, M.F., Souza Mendes, P.R., 1998. Heat transfer to Herschel–Bulkley materials in annular flows. Proc. 7th Brazilian Cong. Thermal Sciences, vol. 2, pp. 1146–1151.

Soares, M., Naccache, M.F., Souza Mendes, P.R., 1999. Heat transfer to viscoplastic liquids flowing laminarly in the entrance region of tubes. Int. J. Heat Fluid Flow 20, 60–67.

Vradis, G.C., Dougher, J., Kumar, S., 1992. Entrance pipe flow and heat transfer for a Bingham plastic. Int. J. Heat Mass Transfer 35, 543–552.

Wilson, S.D.R., 1993. Squeezing flow of a yield-stress fluid in a wedge of slowly-varying angle. J. Non-Newton. Fluid Mech. 50, 45–63.

Wilson, S.D.R., Taylor, A.J., 1996. The channel entry problem for a yield stress fluid. J. Non-Newton. Fluid Mech. 65, 165–176.